© 2018. Published by The Company of Biologists Ltd | Development (2018) 145, dev153692. doi:10.1242/dev.153692

RESEARCH ARTICLE

Trio GEF mediates RhoA activation downstream of Slit2 and coordinates telencephalic wiring

Stéphanie Backer[1,2,*], Ludmilla Lokmane[3,*], Camille Landragin[1,2], Marie Deck[3], Sonia Garel[3] and Evelyne Bloch-Gallego[1,2,‡]

ABSTRACT

Trio, a member of the Dbl family of guanine nucleotide exchange factors, activates Rac1 downstream of netrin 1/DCC signalling in axon outgrowth and guidance. Although it has been proposed that Trio also activates RhoA, the putative upstream factors remain unknown. Here, we show that Slit2 induces Trio-dependent RhoA activation, revealing a crosstalk between Slit and Trio/RhoA signalling. Consistently, we found that RhoA activity is hindered *in vivo* in *Trio* mutant mouse embryos. We next studied the development of the ventral telencephalon and thalamocortical axons, which have been previously shown to be controlled by Slit2. Remarkably, this analysis revealed that *Trio* knockout (KO) mice show phenotypes that bear strong similarities to the ones that have been reported in *Slit2* KO mice in both guidepost corridor cells and thalamocortical axon pathfinding in the ventral telencephalon. Taken together, our results show that Trio induces RhoA activation downstream of Slit2, and support a functional role in ensuring the proper positioning of both guidepost cells and a major axonal tract. Our study indicates a novel role for Trio in Slit2 signalling and forebrain wiring, highlighting its role in multiple guidance pathways as well as in biological functions of importance for a factor involved in human brain disorders.

KEY WORDS: Trio GEF, RhoA, Neuron, Migration, Slit2, Axon guidance, Rho GTPase, Mouse, Embryo, Thalamocortical, Corridor cells

INTRODUCTION

The small guanosine triphosphatases (GTPases) of the Rho family act as relays between the binding of extracellular signalling molecules and cytoskeleton remodelling, to regulate events such as motility and axon outgrowth. Rho GTPases are molecular switches that mostly cycle between an inactive GDP-bound and an active GTP-bound state (Jaffe and Hall, 2005). The control of Rho GTPase nucleotide cycling is mainly performed by two types of regulatory proteins: guanine nucleotide exchange factors (GEFs) enhance the GTP-bound state, whereas GTP hydrolysis is catalysed by GTPase-activating proteins (Tcherkezian and Lamarche-Vane, 2007). Here, we analyse the role of Trio GEF, a large protein of 350 kDa that presents a peculiar structural feature, including two catalytic GEF domains that target small GTPases that have apparent antagonistic downstream activities. The N-terminal Dbl-homology-Pleckstrin-homology (DH-PH) unit (TrioGEF1) mediates GDP to GTP exchange on Rac1 and RhoG, whereas the C-terminal DH-PH unit (TrioGEF2) activates RhoA. Trio is highly expressed in the brain (Portales-Casamar et al., 2006). Recent findings have established the signalling pathways that allow Trio to mediate netrin 1/DCC signalling in axon outgrowth and guidance through the presence and functionality of the GEF1 domain and its ability to activate Rac1 (DeGeer et al., 2015). The role and functionality of the RhoA-GEF2 domain has not been demonstrated, either by using the whole protein *in vitro* (Bellanger et al., 1998; Blangy et al., 2000; Debant et al., 1996) or *in vivo* in mammals. No upstream signalling molecule has been proposed so far to bind Trio to subsequently activate RhoA.

We investigate here the role and partners of Trio in RhoA activation in mammals. RhoA activation downstream of Slit has been proposed to be decisive in the context of repulsive events (Liu et al., 2012). We have investigated whether Trio could be a molecular integrator that could act *in vivo* as a GEF to activate RhoA upon a repulsive guidance cue. Slit2 was chosen as a candidate because it is able to modulate axon outgrowth and neuronal migration guidance. The phenotypic analysis of the development of the central nervous system (CNS) in *Trio* knockout (KO) mice has reported defects in axonal projections, in particular those that form the internal capsule (Briancon-Marjollet et al., 2008). Remarkably, a dramatically abnormal telencephalic phenotype has been reported in a single *Slit2* KO mouse model (Bielle et al., 2011). Thus, based on the detailed mis-wiring in the *Slit2* KO model, we have chosen to focus, in *Trio* KO mice, on the development of thalamocortical axons (TCA) that occurs, in mouse, from embryonic day (E) 12, when they extend ventrally from the thalamus into the ventral telencephalon. Then, TCA turn dorsolaterally to cross the diencephalic-telencephalic boundary at E13. They then reach the internal capsule and fan out, before reaching their appropriate cortical region around E16. Their outgrowth across the subpallium requires the presence of guidepost neurons that are organized as a corridor and called 'corridor cells' (López-Bendito et al., 2006). Corridor cells originate in the lateral ganglionic eminence (LGE) and migrate tangentially in the medial ganglionic eminence (MGE). Slit2 has the ability to orient the migratory path of guidepost neurons and consequently the path of TCA (Bielle et al., 2011).

We show here that, *ex vivo*, the signalling pathway downstream of Slit2 activates RhoA, but it is impaired in the absence of Trio in mouse embryonic fibroblasts (MEFs) that have been freshly obtained from control or mutant embryos of *Trio*$^{+/-}$ littermates. In addition, *in vivo*, the absence of Trio hinders both RhoA and Rac1 activities in the ventral telencephalon in *Trio* KO mice. Remarkably, the analysis of the phenotype of *Trio* KO reveals that guidepost corridor cells are mis-positioned from E12 and pathfinding is

[1]Institut Cochin, Université Paris Descartes, CNRS UMR 8104, 75014 Paris, France. [2]INSERM, U1016, Department of Development, Reproduction and Cancer, 24 rue du Faubourg Saint-Jacques, 75014 Paris, France. [3]Institut de Biologie de l'Ecole Normale Supérieure (IBENS), Ecole Normale Supérieure, CNRS UMR8197, INSERM U1024, PSL research University, 75005 Paris, France.
*These authors contributed equally to this work

‡Author for correspondence (evelyne.bloch-gallego@inserm.fr)

E.B., 0000-0003-2779-6187

Received 21 April 2017; Accepted 24 August 2018

Development (2018) 145, dev153692. doi:10.1242/dev.153692

aberrant in some TCA. There is massive disorganisation, including fasciculated bundles in the ventral telencephalon, which would result from corridor mis-positioning, together with mis-integration of Slit2 guidance cues by TCA along their pathway. Thus, we describe here the sequence that is responsible for abnormal telencephalic development in *Trio* mutant mice, with Trio involved in both the positioning of migrating corridor cells and in guiding TCA pathfinding. Our results demonstrate that Trio is a master integrator for Slit signalling and RhoA activation, in addition to the previously demonstrated netrin 1/DCC/Rac1 signalling. Therefore Trio appears as a bottleneck for transducing guidance cues and cytoskeleton remodelling in the processes of both axon outgrowth and/or pathfinding, and neuronal migration, during embryonic development of the rostral CNS.

RESULTS

RhoA activity is severely decreased in MEFs derived from *Trio*$^{-/-}$ embryos

To decipher the role of Trio in mediating repulsion in response to guidance cues in mammals, we investigated the possible link between Slit/Robo and Trio/RhoA pathways. Recent data from the genetics of *Drosophila* have suggested that repulsion by Robo involves Trio activity (Long et al., 2016). A role for Trio-mediated RhoA activation has been shown in the eye development of chick embryos (Plageman et al., 2011) and was also proposed to affect the innate immune response in *Caenorhabditis elegans* (McMullan et al., 2012).

We therefore analysed the level of RhoA activity in control or Slit2-treated MEFs that had been freshly dissociated from control or *Trio* KO E14-18 embryos (Fig. 1A). We first ensured that Trio was properly expressed in control MEF extracts (Fig. S1A). Trio can encode several isoforms as a result of alternative splicing. In control MEF extracts, Trio antibodies mainly detected a doublet that is likely to correspond to Trio D (300 kDa) and Trio A (250 kDa), two splice variants that have previously been reported to be expressed in the CNS (Schmidt and Debant, 2014). Although faint, the full-length form of Trio (migrating at around 350 kDa) was also detected (Fig. S1A, left panels). None of these Trio isoforms could be detected in *Trio*$^{-/-}$ MEFs. We also ensured that both control and *Trio*$^{-/-}$ MEFs properly express Robo1 and/or Robo2 receptors (Fig. S1A, right panels).

Before Slit2 stimulation, the basal level of RhoA activation was comparable in both wild-type (WT) and *Trio* KO MEFs (Fig. 1A, upper left panels). In WT MEFs, Slit2 treatment led to a transient increase in the level of RhoA GTP: a significant stimulation was detected after 5 min of treatment (**P<0.001), whereas it had returned to around its original level by 15 min. In contrast, no increase of RhoA activation was observed in *Trio*$^{-/-}$ MEFs (Fig. 1A, upper right panel). This indicates that the transient activation of RhoA upon Slit2 stimulation observed in control MEFs is dependent on the presence of Trio.

As Trio was previously shown to be able to activate Rac1 in response to netrin 1 (Briancon-Marjollet et al., 2008),

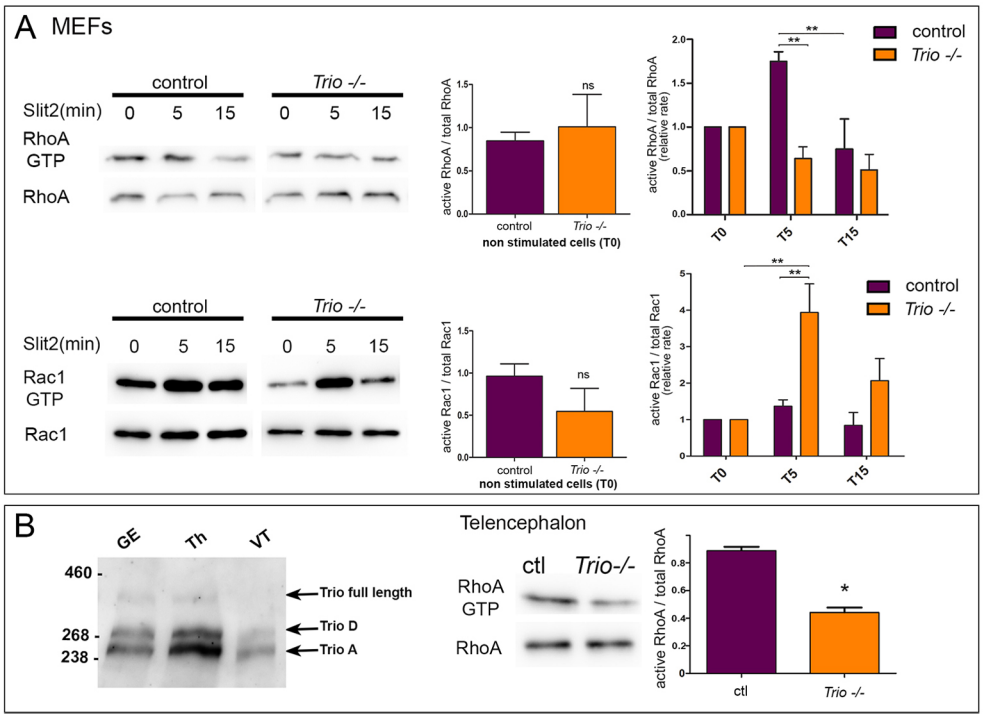

Fig. 1. Trio is required to mediate RhoA activation upon Slit2 stimulation, Rac1 activation occurs only in the absence of Trio. (A) Western blot (left panels) and quantification (right panels) of RhoA activity (top) or Rac1 activity (bottom) following Slit2 stimulation of MEFs obtained from control WT animals (RhoA controls, n=4; Rac1 controls, n=3) or from *Trio*$^{-/-}$ mutant mice (RhoA, n=4; Rac1, n=3) for different periods of time. Upon a 5 min Slit2 stimulation, the activity of RhoA is increased but is strictly dependent on the presence of Trio, whereas Rac1 activation in MEFs is significantly increased after a 5 min Slit2 stimulation, exclusively in the absence of Trio. The activation states are compared between paired MEF samples from control and *Trio*$^{-/-}$ animals of the same litters. ** P<0.001 (two-way ANOVA with Bonferroni's multiple comparison test). ns, not significant (P>0.05). Error bars are s.e.m. (B) The full length Trio (350 kDa) is slightly detected in ventral telencephalon (VT) extracts in a western blot (left panel). Trio is mainly expressed as spliced isoforms migrating as a doublet, which is likely to correspond to Trio D (300 kDa) and Trio A (250 kDa), as well as in ganglionic eminences (GE) and thalamus (Th) extracts. Right panel shows western blot and quantification of the relative active state of RhoA, after pull-down assays using GST-Rhotekin and ventral telencephalon extracts from E14 WT (ctl, n=3) mice and *Trio*$^{-/-}$ mice (n=3). The activation states are compared between paired control and mutant animals of the same litters. Four different littermates have been used for this experiment. *P=0.019 (Student's t-test). Error bars are s.e.m.

Development (2018) 145, dev153692. doi:10.1242/dev.153692

we investigated whether Slit2 could activate Rac1 in a Trio-dependent manner in MEFs. We therefore analysed the rate of Rac1 activation upon Slit2 stimulation of WT and *Trio*$^{-/-}$ MEFs (Fig. 1A, bottom panels). Although the rate of Rac1 activation after a 5 min Slit2 treatment was low in control MEFs, it increased significantly after Slit2 stimulation of *Trio*$^{-/-}$ MEFs (**P<0.001). This assay thus revealed that the absence of Trio, instead of preventing Rac1 activation in response to Slit, induces or facilitates its activation. These data show that the presence of Trio is required for RhoA activation after Slit2 stimulation, but it antagonizes Rac1 activation, illustrating a possible physiological Rho-Rac antagonism that could involve Trio GEF (see Discussion).

Trio is expressed in the ventral telencephalon and thalamic region during development and it regulates RhoA activity *in vivo*

We next aimed to determine whether Trio modulates RhoA activity *in vivo*. Therefore, we first examined whether *Trio* shows a specific transcript expression in the embryonic brain, by performing *in situ* hybridization (ISH) from E12.5 to birth (Fig. 2). We observed a very broad expression in the neocortex and ventral telencephalon mantle at E12.5 (Fig. 2A,B). The labelling was detected in the mantle layer of both LGE and MGE, but low in their ventricular and subventricular zones (asterisks). *Trio* transcripts were also detected in striatum, diagonal and preoptic zones, whereas its expression is low rostrally in the pallium (not shown). At E14.5 (Fig. 2C,D), *Trio* was strongly expressed in the thalamus and in the ventral part of the telencephalon (Fig. 2C), as well as in the neocortex cortical plate. At birth (P0, Fig. 2E,F), *Trio* transcripts were present in the striatum, hippocampus and neocortex. In the hippocampus, the subiculum, the dorsolateral part of the pre/parasubiculum and the adjacent region of the cingular anterior and infralimbic cortex express *Trio*. Notably, ISH probes, including the full-length *Trio* transcripts or restricted to the GEF-2 domain [present in all Trio isoforms except Trio B and C (Schmidt and Debant, 2014)], showed a similar expression pattern. Consistent with these ISH data, western blot analyses detected the Trio protein in the ventral telencephalon, the ganglionic eminences and the thalamus. All three tissues mainly expressed Trio D (300 kDa) and Trio A (250 kDa) isoforms, but very low levels of full-length Trio (Fig. 1B, left panel).

We thus focused our functional studies on the ventral telencephalon, a structure that has been previously shown to be perturbed in *Trio* KO mice (Briancon-Marjollet et al., 2008) and to be responsive to Slit2 signalling (Bielle et al., 2011). Pull-down assays using whole ventral telencephalon extracts at E14.5 revealed a greater than twofold decrease in activated/total RhoA ratio in *Trio*$^{-/-}$ compared with WT extracts (n=4 independent experiments, *P=0.02 Fig. 1B). Attempts to further stimulate RhoA activity with Slit2 on dilacerated telencephalon were not successful, possibly because of technical aspects or to a constitutive activation by endogenous Slit2. Nevertheless, together with our *ex-vivo* data that revealed the lack of RhoA stimulation upon Slit activation in *Trio*$^{-/-}$ MEFs, this endogenous decrease in active (GTP-bound) RhoA in the absence of Trio is consistent with a role of Trio in RhoA activation downstream of Slit2 *in vivo*.

Netrin 1, Slit and Robo receptors remain properly expressed in the absence of Trio

As Rho has been linked to the transcriptional machinery through the Rho-serum response factor (SRF) connection (Settleman, 2003), we ensured that the absence of Trio that affects Rho activation in the

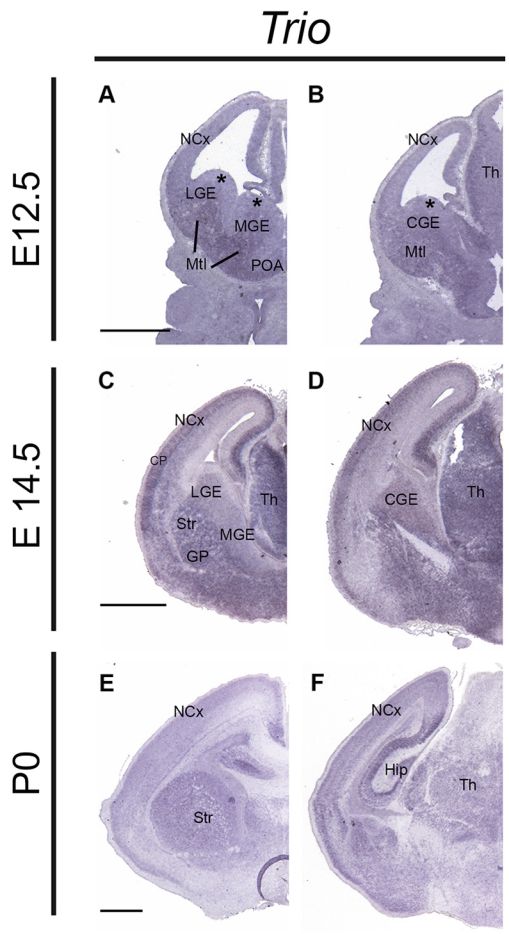

Fig. 2. Expression of *Trio* transcripts in mouse telencephalon and thalamus at E12.5, E14.5 and at birth. (A-F) ISH showing *Trio* transcript expression in the embryonic brain. At E12.5, *Trio* expression is located in the mantle layer of both LGE and MGE, whereas it is absent in the ventricular and subventricular zones of both (asterisks) (A,B). At E14.5, *Trio* is strongly expressed in the thalamus and in the ventral region of the telencephalon, including the striatum, and in the mantle of MGE, LGE and caudal ganglionic eminence. A strong *Trio* expression is also observed in the subcortical plate of the neocortex (C,D). At birth (P0), *Trio* transcripts are present in other regions, in the striatum and the thalamus (E,F). CGE, caudal ganglionic eminence GP, globus pallidus; Hip, hippocampus; Mtl, mantle layer; NCx, neocortex; Str, striatum; Th, thalamus. Scale bars: 500 µm.

telencephalon (Fig. 1B) does not affect cell synthesis of guidance cues. At E14.5, ISH with either *Slit2* or netrin 1 (*Ntn1*) probes were performed in control and *Trio*$^{-/-}$ mutants. In the absence of *Trio* (Fig. 3E), *Ntn1* remains expressed as previously reported and as illustrated in WT animals here (Fig. 3A), i.e. in the ventricular zone of the LGE, in the whole striatum and in the most basal part of the telencephalon, including the globus pallidus. *Slit2* also remains similarly expressed in both WT (Fig. 3B,B′) and *Trio*$^{-/-}$ (Fig. 3F,F′) mice, both in localization and intensity, i.e. at a high level in the ventral midline. The expression domains of Robo receptors remain roughly identical in control (Fig. 3C and D for *Robo1* and *Robo2*, respectively) and mutant *Trio*$^{-/-}$ (Fig. 3G and H for *Robo1* and *Robo2*, respectively) in thalamic (not illustrated) and telencephalic regions. In both control and mutant embryos, *Robo1* and *Robo2* transcripts are expressed in a partially complementary manner in the thalamus, and both receptors are expressed in the striatum. *Robo2* labelling is intense and localized in the striatal region, whereas *Robo1* labelling shows a more diffuse aspect in the mantle zone.

Development (2018) 145, dev153692. doi:10.1242/dev.153692

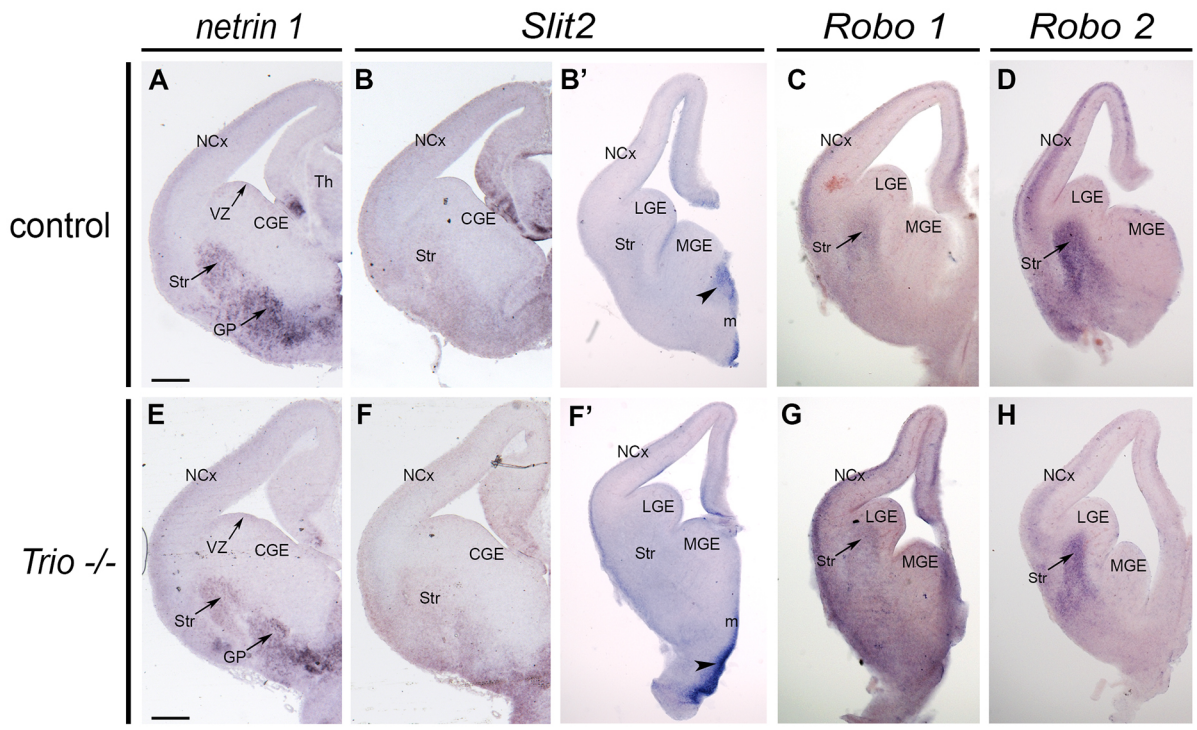

Fig. 3. Expression domains of netrin 1, Slit2, Robo1 and Robo2 transcripts in E14.5 control and *Trio*$^{-/-}$ embryos. (A-H) Coronal sections through mid-telencephalic/rostral diencephalic levels of E14.5 control and *Trio*$^{-/-}$ embryos used to analyse the expression of *Ntn1* (A,E) and *Slit2* (B,B′,F,F′) mRNAs using cryosections, and of *Robo1* (C,G) and *Robo2* (D,H) using vibratome sections. At E14.5, in the absence of *Trio* (E), the ventricular zone of the LGE, the whole striatum in the mantle zone and the most dorsal part of the thalamus still express *Ntn1* transcripts as in control animals (compare A with E). *Slit2* transcripts are visualized after ISH in control (B,B′) and *Trio*$^{-/-}$ (F,F′) embryos: the ventral midline and the ventricular zones of the LGE and MGE (B′,F′) express *Slit2* mRNAs. Arrowheads indicate *Slit2* expression in the ventral midline. *Robo1* (C,G) and *Robo2* (D,H) transcripts remain expressed in identical areas in both control (C,D) and *Trio*$^{-/-}$ (G,H) E14.5 embryos: in the neocortex and dorsal thalamus (not illustrated) in a partially complementary manner, and in the mantle, but with a higher expression level for *Robo2*. CGE, caudal ganglionic eminence; GP, globus pallidus; m, ventral midline; NCx, neocortex; Str, striatum; Th, thalamus; VZ, ventricular zones. Scale bars: 200 µm.

Robo1 expression is further assessed by western blot, in E13 cortical and thalamic extracts, and in ventral telencephalon extracts at E14 (Fig. S1B).

Corridor guidepost cells show a defective positioning

Because our data suggested that Trio acts downstream of Slit2 *in vivo*, we next compared the phenotypes of *Trio* KO mice with the ones that have been reported in *Slit2* KO mice (Bielle et al., 2011). In particular, it has been demonstrated that Slit2 is required for proper development of the telencephalon, notably for the positioning of corridor cells (López-Bendito et al., 2006; Bielle et al., 2011).

Corridor cells migrate tangentially from the LGE at E12 into the MGE, and guide the path of TCA at E13.5 (López-Bendito et al., 2006). Corridor cells were visualized with an *Ebf1* ISH probe, which also labels the striatum (Fig. 4). From E12.5 (n=2), in mutant mice (Fig. 4B) *Ebf1*-expressing cells formed an abnormal horizontal 'beak', which contrasts with the continuous appearance of the migratory stream in WT embryos (Fig. 4A). At E14.5 (n=5), the geometry of the *Ebf1*-positive corridor between the LGE and MGE was still strikingly compacted in mutant mice, with some cells mis-oriented towards the MGE instead of migrating more ventrally (Fig. 4D), compared with the regular organization that was observed in control embryos of the same stage (Fig. 4C). Striatal defects were also observed at E18.5 (n=3; not shown). Interestingly, the corridor was similarly distorted and oriented towards the midline in *Slit2* KO mice (Bielle et al., 2011). Altogether, these phenotypic observations in *Trio* mutant mice reveal that the positioning of corridor cells is impaired, which could affect the TCA navigation, as has been reported in *Slit2* KO mice (Bielle et al., 2011).

Abnormal outgrowth and pathfinding of TCA in *Trio* KO

Invasion of the striatum and cortex by TCA depends on the positioning of corridor cells and has been reported to be delayed in *Slit2* KO mice (Bielle et al., 2011), whereas it is premature in *Robo1* KO mice (Bielle et al., 2011). We therefore analysed TCA pathfinding using both immunostaining and axonal tracing by carbocyanine injections. To analyse the development of axons, L1 immunoreactivity was used to visualize thalamocortical fibres. At E14.5, in *Trio* mutants (n=5) TCA appeared to have a delayed outgrowth through the striatum and showed misguided bundles. The progression of axons was stalled ventrally in the mutant ventral telencephalon (Fig. 5E), whereas in controls (n=5), TCA had already crossed this structure and reached the neocortex (Fig. 5A). Analysis of TCA at E18.5 using L1 immunostaining (n=3; Fig. 5I, M) revealed that axons had reached the neocortex in *Trio* mutants (Fig. 5M), but that they were forming disorganized bundles across the striatum, in contrast to their fan shape in control animals (Fig. 5I). Thus TCA outgrowth and trajectory were impaired between E14.5 and E18.5 in the absence of Trio.

The proper pathfinding of TCA when they emerge from the thalamus and navigate through the internal capsule regulates their initial direction towards neocortical regions (Lokmane et al., 2013). We thus further analysed the respective pathways of motor and somatosensory TCA, originating from the ventro-lateral thalamus (VL) and the ventro-posterior (VP) nuclei, respectively

Development (2018) 145, dev153692. doi:10.1242/dev.153692

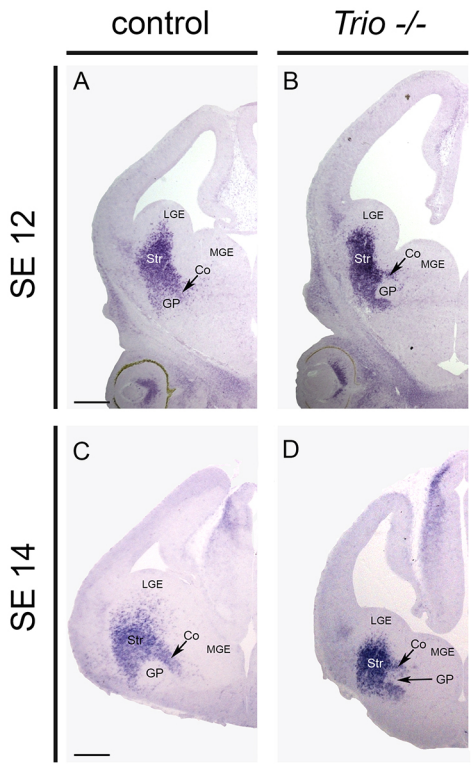

Fig. 4. Guidepost cells fail to position properly from the LGE to the MGE to set up the corridor in *Trio*$^{-/-}$ mice. (A-D) ISH visualization of *Ebf1* expression in corridor cells (Co) and striatum (Str). The shape of the corridor cell migratory path is abnormal in *Trio*$^{-/-}$, both at E12.5 (n=2 for both mutant and control, compare B with A) and at E14.5 (n=5, for both mutant and control, compare D with C). The migratory path is compacted, shortened and mis-oriented in the absence of Trio. GP, globus pallidus. Scale bars: 200 µm.

(Lokmane and Garel, 2014). At E16.5, anterograde tracings by double 1,1′-dioctadecyl 3,3,3′,3′-tetramethylindocarbocyanine perchlorate (DiI) and 4-4-dihexadecyl aminostryryl N-methyl-pyridinium iodide (DiA) injections in the VP and VL nuclei respectively show that TCA organization is severely impaired in mutants (n=3; Fig. 5F-H). Indeed, in controls (n=3; Fig. 5B-D) VL motor and VP somatosensory TCA reached the neocortex with a stereotyped compact trajectory through the ventral telencephalon: VL axons were more dorsal in the internal capsule than the VP TCA. In *Trio* mutants, VP somatosensory axons (compare Fig. 5F-H with Fig. 5B-D) progressed as a larger and disorganized bundle when crossing the ventral telencephalon, although some axons succeeded in reaching the neocortex at E16.5. In contrast, motor projections that arose from the VL nucleus (compare Fig. 5F-H with Fig. 5B-D) avoided crossing the ventral telencephalon and remained blocked caudally in the ventral telencephalon, not reaching the neocortex.

Finally, by retrograde tracing at E18.5 after double injections of DiA in motor (M1) and DiI in somatosensory (S1) neocortex (Fig. 5J-L and N-P), we monitored the topographic projections of TCA. In WT animals, double injections clearly show the stereotyped exclusive path of motor and somatosensory axons through the ventral telencephalon as well as the retrolabelling of thalamic neurons in specific nuclei (n=5; Fig. 5J-L). In mutant embryos (n=3, Fig. 5N-P), DiI injections in S1 led to a retrolabelling in the thalamus that indicated the TCA did reach S1. Furthermore, axonal labelling in the ventral telencephalon revealed that at E18.5, as at E16.5, somatosensory TCA are disorganized. In the mutant, DiA injections in M1 show axonal labelling in the dorsal striatum, but not in the internal capsule or the thalamus. The variation in the dispersion of the thalamic axonal tract, quantified in either WT or *Trio*$^{-/-}$ mutant embryos, reflects the disorganized outgrowth and guidance of TCA, which is less constrained in the absence of Trio (Fig. 5Q).

Our analyses thus indicate that: (1) the trajectory of growing TCA is affected when they reach the ventral telencephalon, showing delayed outgrowth and enlarged fascicles in the absence of *Trio*; (2) some somatosensory TCA reached the neocortex via aberrant and ectopic pathways in *Trio* mutants, whereas motor TCA were more severely affected and did not reach the neocortex.

Impaired collapse responses to Slit2 in dissociated thalamic neurons from *Trio* KO

To further analyse the functional link between Slit2 signalling and Trio function, we performed collapse assays by treating E13.5 dissociated thalamic neurons from either WT (n=5, Fig. 6A-F) or *Trio* mutant (n=6, Fig. 6G-L) embryos from three different littermates with Slit2 (Fig. 6). We scored the number of collapsed versus non-collapsed thalamic axon growth cones, either without stimulation (WT, n=403; *Trio*$^{-/-}$, n=419) or 20 min after Slit2 stimulation (WT, n=395; *Trio*$^{-/-}$, n= 354). The rate of collapsed growth cones (25%) in *Trio*$^{-/-}$ thalamic axons is higher than in WT (17%) in basal conditions without stimulation (**P<0.008). Nevertheless, whereas Slit2 treatment induced a twofold increase of collapsed growth cones from WT thalamic neurons (16 to 35% collapse; ****P<0.0001, Fig. 6M), the ratio of collapsed growth cones was not significantly increased in *Trio*$^{-/-}$ thalamic axons (29% after Slit2 treatment versus 24% in basal conditions). These results indicated that in the absence of Trio, growth cones have lost their ability to collapse in response to Slit2. Thus, Trio appears to be important to mediate Slit2-driven growth cone collapse.

In conclusion, our detailed anatomical analysis of *Trio*$^{-/-}$ mutants showed that, although not strictly identical in extent, *Trio* phenotypes are coherent and correlate with several striking observations that have been previously reported in *Slit2* KO mice. In addition, the efficiency of Slit2 treatment for inducing growth cone collapse on dissociated thalamic neurons strongly depends on the presence of Trio. Finally, RhoA is activated upon Slit2 treatment in WT MEFs but not in *Trio*$^{-/-}$ MEFs. Thereby, both *in vivo* and *in vitro* assays strengthen the possibility that Trio, in addition to its established function downstream of netrin 1, interacts with Slit2 signalling.

DISCUSSION

This work participates in filling in the missing links that surround Trio in the network of molecular interactions that control RhoA activation. It also demonstrates a crucial role of Trio downstream of Slit2. We report here that RhoA activity is increased upon Slit2 treatment in a Trio-dependent manner. *In vitro* and *in vivo*, RhoA activity is impaired in the absence of Trio. In addition, the collapsing activity of Slit2 on TCA is lost in the absence of Trio. Thus, we demonstrate here that Trio belongs to a signalling cascade downstream of the guidance cue Slit2 that can induce RhoA activation *in vivo*. The development of the forebrain, in particular the development of the ventral telencephalon and TCA, was previously shown to be controlled by Slit2 and we have analysed these structures in *Trio* mutants. The phenotype we observed in *Trio* mutants is similar to the one that has been reported by us and others in *Slit2* mutants (Bielle et al., 2011) in the following respects: (1) TCA are ventrally mis-routed at the telencephalic/diencephalic boundary; (2) TCA have an abnormal ventral route through the

Development (2018) 145, dev153692. doi:10.1242/dev.153692

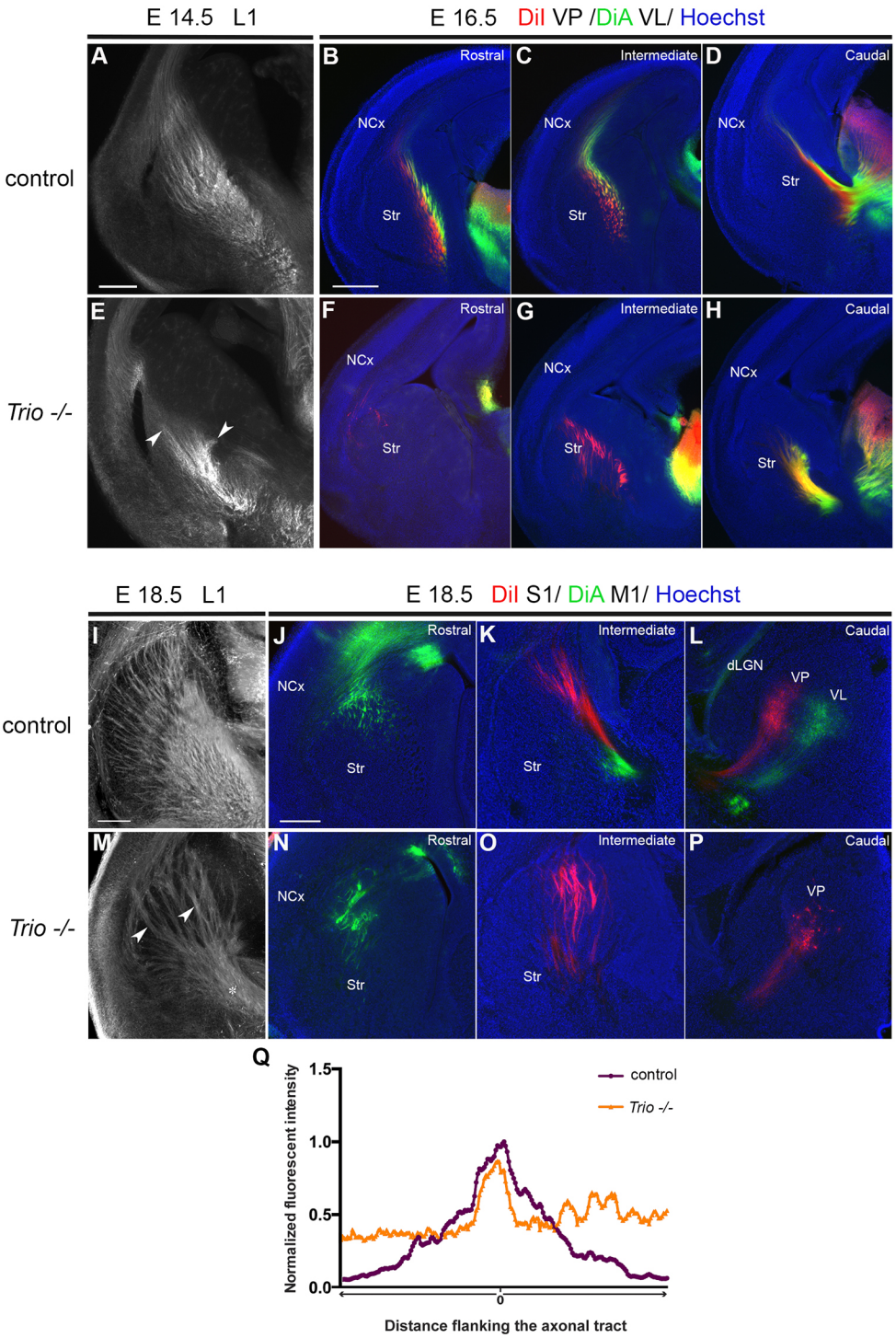

Fig. 5. TCA pathfinding is compromised in *Trio*$^{-/-}$ embryos. (A-P) L1 immunostaining and axonal labelling of control and *Trio*$^{-/-}$ mutant mice from E14.5 to E18.5. L1 immunostaining of TCA trajectories at E14.5 (A,E) and E18.5 (I,M). In *Trio*$^{-/-}$ mutants, axons are compacted, forming bundles across the striatum, contrary to their fan-shape spread in the control. At E14.5 TCA are ventrally confined in *Trio* mutant mice (E, *n*=5), not showing the rostral reorientation across the striatum that is observed in control mice (A, *n*=5). The striatum is abnormally shaped and perforated by TCA bundles at E14.5 and E18.5 (*n*=3) in the absence of *Trio*. Arrowheads indicate axon bundles in *Trio*$^{-/-}$ mutants. Injections of DiI in the ventro-posterior nucleus of the thalamus and DiA in the ventro-lateral thalamus at E16.5 show that in E16.5 (B-D, *n*=3) WT forebrains, TCA cross the subpallium and form a compact internal capsule with TCA growing in the striatum, and a linear organization of axon fascicles to reach the cortical subplate, whereas the axonal trajectory is severely affected in *Trio*$^{-/-}$ mutants and few of them reach the neocortex (F-H, *n*=3). Axonal labelling at rostral, intermediate and caudal levels of the brain after injection of carbocyanines crystals in the E18.5 neocortex, DiA in M1 (green) and DiI in S1 (red), shows that motor and somatosensory axons follow a stereotyped trajectory through the subpallium in WT mice (J-L, *n*=5). Retrograde tracing at E18.5 allows the anterograde labelling of the reciprocal corticothalamic axons (CTA). In *Trio*$^{-/-}$ (N-P, *n*=3), DiA injection at a rostral level shows that CTA grow out of the neocortex and invade the striatum but then stop, whereas DiI injection reveals the disorganized trajectory through the subpallium as well as a retrolabelling in the thalamus, indicating that TCA can reach the neocortex. dLGN, dorsolateral geniculate nucleus; NCx, neocortex; Str, striatum; VL, ventro-lateral thalamus; VP, ventro-posterior nucleus of the thalamus. Scale bars: 200 µm in A,E; 250 µm in B-D,F-P. (Q) Quantification of the dispersion of the thalamic tracts at E18.5 using ImageJ showing that the TCA trajectory is more spread in the *Trio*$^{-/-}$ subpallium compared with the control, in which TCA follow a specific path.

telencephalon; (3) TCA that reach the neocortex show topographic defects; (4) the positioning of corridor cells is abnormal, which could be at least partly responsible for the defects in TCA outgrowth, guidance, and projections.

It is noteworthy that *Ntn1* or *DCC* mutants did not show a ventral mis-routing of TCA, nor show defects in corridor cell positioning (Bielle et al., 2011; Braisted et al., 2000; Castillo-Paterna et al., 2015; Powell et al., 2008). They showed a difference in the speed of TCA progression and minor topographical organization defects, which is in sharp contrast with the profound abnormalities observed in *Trio* KO mice.

Taken together, our results indicate that the phenotype observed in *Trio* mutants shows striking similarities to the one observed in *Slit2* mutants, and is much more severe than the one observed in *Ntn1/DCC* KOs. As such, our results support a potential role for Trio downstream of Slit2 in this system.

We therefore report a major and novel role of Trio in ensuring both the signalling pathway downstream of Slit2 and the proper wiring of the telencephalon, by guiding both corridor cell positioning and TCA pathfinding. In this integrative developmental process, Trio would confer the positional guidance information necessary for neuronal positioning and

Development (2018) 145, dev153692. doi:10.1242/dev.153692

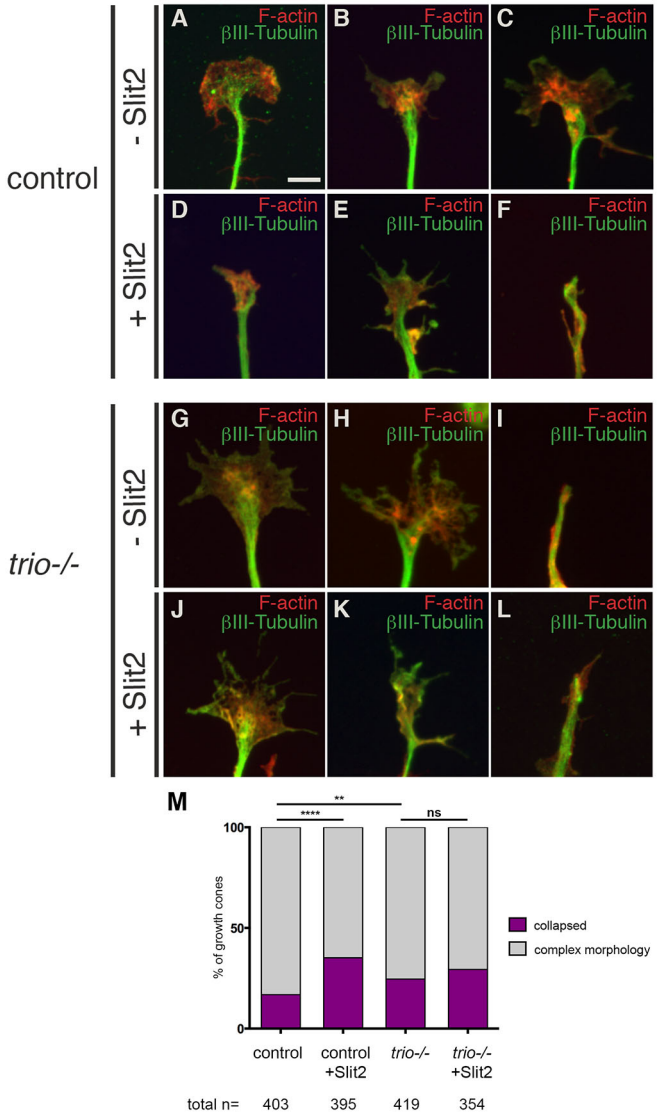

Fig. 6. Slit2-induced collapse of thalamic growth cones depends on the presence of Trio. (A-L) Collapse assays on E13.5 dissociated thalamic neurons from WT (A-F) or *Trio*$^{-/-}$ embryos (G-L) in the presence (D-F and J-L) or absence (A-C and G-I) of Slit2. Phalloidin (for F-actin) and Tuj1 (for βIII-Tubulin) double staining allows visualization of the complex morphologies of growth cones or their collapsed aspect (as observed in F,I,L). Scale bars: 5 µm. (M) Quantification of collapse were performed with five WT and six *Trio*$^{-/-}$ mutants from three distinct littermates. For each condition, the total number of growth cones analysed is indicated. Note that unlike in WT neurons, the percentage of axonal growth cones collapsing is not significantly increased in response to Slit2 in *Trio*$^{-/-}$ thalamic neurons. ns, $P>0.05$, ****$P<0.0001$ and **$P<0.008$ (Fisher's exact test).

axon ordering to the cytoskeleton, which are required for the proper adult cytoarchitecture.

So far, Trio had been mainly studied and proposed to act downstream of netrin 1 (Schmidt and Debant, 2014), and it has been shown to mediate Rac1 activation and axon outgrowth and guidance in response to netrin 1 (Briancon-Marjollet et al., 2008). Furthermore, along with the netrin 1/DCC/Trio signalling pathway, the phosphorylation of Trio has been reported to be essential for Rac1 activation by netrin 1 and for the proper targeting of DCC to the cell surface of growth cones, in order to mediate netrin 1-induced axon outgrowth (DeGeer et al., 2013). The present study demonstrates that Trio also participates in an additional signalling pathway including Slit/(Robo)/Trio/RhoA. Future studies will however be required to determine whether this pathway directly involves Robo and its intracellular domain binding to Trio upon stimulation by Slit2. Robo1 and/or Robo2 may not be the unique Trio partner downstream of Slit2 (Fig. 7).

Our results also show that RhoA, and not Rac1, stimulation by Slit2 is strictly Trio dependent, whereas a very significant Rac1 activation by Slit2 only occurs in cells devoid of Trio-GEF activity. Trio thus appears to be involved in the regulation of a possible physiological Rho-Rac antagonism. Interestingly, the modifications of the growth cone shape result from, among other factors, variations of Rho and Rac activities. We report here that the rate of collapsed growth cones in *Trio*$^{-/-}$ thalamic axons is higher than in WT in basal conditions *in vitro* (Fig. 6), suggesting that Trio may be necessary to prevent some spontaneous thalamic growth cone collapse. Thus Trio may act as a mediator between RhoA and Rac1 pathways to promote the reciprocal inhibitory relationship between both GTPases, as has been previously deciphered for a class of GTPase-activating proteins, FilGAPs (Nakamura, 2013).

Recent literature has now well established that extracellular interactions and crosstalks between various guidance cues are required to direct axon guidance and neuronal migration during embryonic development (Chen, 2018). However, the signalling pathways that allow the integration of their respective or combined effects to reorganize the cytoskeleton remain poorly characterized.

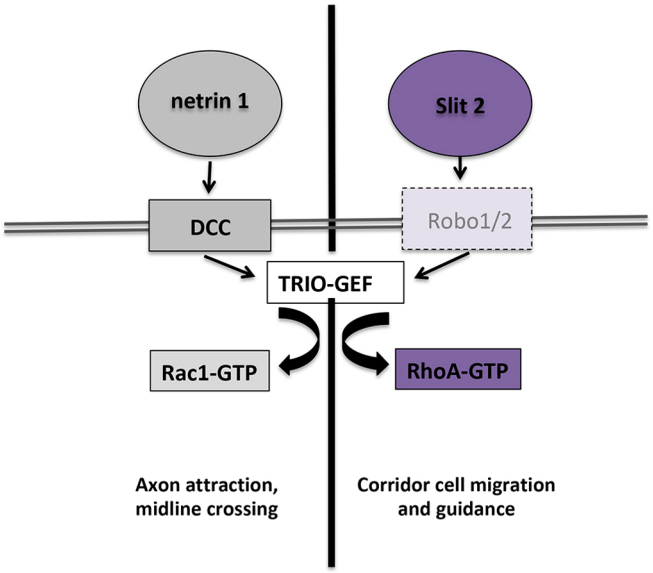

Fig. 7. Trio as a possible bottleneck: a model of the integrative signalling pathway. Trio-GEF carries two GEF domains. The GEF1 domain has already been shown to be activated downstream of netrin 1 binding on DCC receptors in mammals, it allows axon attraction, and this pathway also allows axons to cross the midline. The present data demonstrate that Slit2 is able to stimulate RhoA activation during mouse telencephalon embryonic development. Thus Trio acts a master integrator for Slit/RhoA signalling through Trio/RhoA/GEF activity, in addition to netrin 1/DCC/Rac1 activation through its Trio/Rac1/GEF activity. Whether the Slit/RhoA pathway involves exclusively, or not, Robo receptors that are expressed in the telencephalic regions (Fig. 3 and Fig. S1B) remains to be determined. Therefore Trio is a bottleneck for transducing guidance cues and cytoskeleton remodelling in the processes of both axon outgrowth/pathfinding and neuronal migration during embryonic development of the rostral CNS. The signalling pathway that allows RhoA activation downstream of Trio-GEF is functional *in vivo* and it allows the proper migration and positioning of corridor cells.

Development (2018) 145, dev153692. doi:10.1242/dev.153692

We reveal here that Trio can activate RhoA *in vivo* downstream of Slit2 and could act as a molecular bottleneck to integrate both Rho and Rac signalling downstream of Slit2 and netrin 1, respectively.

RhoA activation downstream of Slit has been proposed to be decisive in the context of repulsive events. It is, in particular, the case for the dispersion of oligodendrocyte precursors (Liu et al., 2012). We report here that Trio is strictly required to activate RhoA downstream of Slit2 stimulation in MEFs and *in vivo*. Activation of the Rho GTPases Rac and Cdc42 promotes the formation of lamellipodia and filopodia, respectively (Lawson and Burridge, 2014), whereas activation of the Rho family member RhoA leads to increased actomyosin contractility, growth cone collapse or cell dispersion. Thus, Rac and Cdc42 activation would mimic attractive axon guidance cues, whereas Rac and Cdc42 inhibition or RhoA activation mimics repulsive cues, and Trio could mediate the effects of repulsive cues. Trio/RhoA are required for neuronal positioning of guidepost cells in response to Slit2, which ensures TCA outgrowth (see schematic in Fig. 7). The precise effect of Slit2 on corridor cell positioning remains to be analysed; it could possibly affect their oriented migration or the efficiency of their migration.

It will be interesting to determine the specific functional domains of Trio that are involved and regulated during the respective activation of both Rac1 and RhoA, and that allow Trio to integrate signalling of different guidance cues to remodel the cytoskeleton. It has been shown that RhoGEF can be regulated by protein-protein or intramolecular interactions. Their activity can also be dependent on their subcellular localization, either membrane targeted or sequestered in the nucleus (Cherfils and Zeghouf, 2013). *In vivo*, it would be interesting to define ultrastructurally conformational changes of Trio that can occur in the growth cone leading processes and in cell bodies, which could allow the accessibility and activity of either GEF1 and/or GEF2.

Other GTPase regulators of the actin cytoskeleton have been studied for their inhibitory action on small Rho GTPases (Rac1, RhoA and Cdc42) downstream of Slit. Slit-Robo GTPase activating proteins (srGAP1, srGAP2 and srGAP3) were identified in a two-hybrid screen as downstream components of the Slit/Robo pathway in forebrain neuroblasts, and Rac1 inhibition has been proposed as a major consequence of srGAP recruitment. SrGAP3/MEGAP is a member of the srGAP family and is implicated in repulsive axon guidance and neuronal migration through Slit-Robo-mediated signal transduction. It has been shown to be part of the Slit-Robo pathway that regulates neuronal migration and axonal branching (Wong et al., 2001). Although still to be demonstrated, Slit2 effects are at least partly linked to Cdc42 inactivation by srGAP1. In the context of guidance cues and to reconcile our observations and these results, it is plausible that either GAPs or GEFs lead to a specific balance of activity to modulate Rho GTPases, GEF specificity resulting also from their localization and from the presence of appropriate molecular partners.

The phenotypic analyses of *Trio* mutants demonstrate that the loss of Trio signalling leads to abnormal TCA navigation and defective wiring of the neocortex, suggesting a crucial role of Trio in orchestrating both guidepost cell migration, TCA outgrowth and somatotopic cortical projections. Trio appears to be involved in wiring both motor and somatosensory projections. Moreover the anterior commissure has been reported to be absent in *Trio* null embryos, and netrin 1/DCC-dependent axonal projections that form the corpus callosum have also been reported to be defective in the mutants (Briancon-Marjollet et al., 2008). We have also observed that the lateral olfactory tract (LOT) is abnormally shaped in the absence of Trio and the pathfinding of the LOT is impaired in the mutant compared with the control (not illustrated). It is remarkable that the proper development of the LOT is similarly a function of the proper positioning of guide cells (LOT cells) and it involves the Slit/Robo pathway (Fouquet et al., 2007; Nguyen-Ba-Charvet et al., 2002). We suggest that Trio is an appropriate master integrator to regulate both tangential migration and axon outgrowth *in vivo* during mouse embryogenesis. We have previously shown that neuronal migration depends on the Rho/ROCK pathway, whereas axon outgrowth depends on Rac1 activation (Causeret et al., 2004). Thus Trio could regulate axon outgrowth and neuronal migration through both its functional GEF domains.

Interestingly, *TRIO* has been recently marked as a candidate gene for intellectual disability (ID) as four truncating monoallelic mutations have been identified in patients that have been reported to have mild to borderline ID combined with behavioural problems (Ba et al., 2016). It is noteworthy that heterozygous nonsense mutations have been reported in humans. Although recorded with ID, clinical exams also reveal motor deficits. In addition to *TRIO* mutations in cases of ID with both cognitive and motor defects, novel *de novo* genetic damage to both GEF domains that altered TRIO catalytic activity have been recently proposed to contribute to neurodevelopmental diseases (ADS, schizophrenia, bipolar disease and intellectual disability) (Katrancha et al., 2017; Sadybekov et al., 2017). Combining this report and our observations, it will be interesting to determine whether these patients carrying *TRIO* mutations show thalamic malformations or defective forebrain wiring, with impaired thalamocortical or reciprocal corticothalamic connections (Ba et al., 2016). It will also be of interest to investigate whether monoallelic mutations in either *Slit*, *Robo* or *Trio* could lead to similar syndromes, as they affect a common signalling pathway, by targeted sequencing of Slit1 and/or Slit2, and Robo1 and/or Robo2, in over 2300 individuals who have been diagnosed with ID. In parallel, it will be worth testing whether heterozygous mice carrying a monoallelic *Trio* mutation develop sensory or motor inabilities.

Remarkably, abnormal neuronal apoptosis has been reported in cases of mental retardation and/or lissencephaly (Di Donato et al., 2016). Our preliminary data reveal that apoptotic figures are rare events in the developing CNS devoid of Trio, but caspase-positive areas have been detected between E15.5 and birth in thalamic nuclei, whereas none have been detected in the ventral telencephalon. Note that, despite anatomic mis-organizations in the hindbrain (Backer et al., 2007) and spinal cord, no apoptotic figures were reported. Whether wiring defects in the absence of *Trio* may lead to apoptosis remains to be characterized.

Taken together, our data demonstrate a novel role for Trio acting downstream of Slit2 and activating RhoA. These results strongly suggest that Trio can act as a molecular integrator of complementary positional and guidance information to allow axon ordering during embryogenesis, and to control the formation of the topographic map, in particular in the mature forebrain.

MATERIALS AND METHODS

Animals

Pregnant Swiss mice were purchased from Janvier Laboratories. Timed matings of *Trio*$^{+/-}$ mice (O'Brien et al., 2000; BALB/c genetic background) were used to obtain embryos at different developmental stages. The day of the vaginal plug was considered E0.5. DNA was isolated from the tail and used for genotyping with appropriate primers. Animals were handled in accordance with French and European regulations and approved by the Paris Descartes (CEEA 34) ethical committee for animal experimentation, in accordance with the information provided by the French Ministry of Research.

Fixation

Mouse embryos were obtained from timed mating of outbred Swiss mice or from heterozygous *Trio* mutant mice (O'Brien et al., 2000). Mouse embryos

Development (2018) 145, dev153692. doi:10.1242/dev.153692

between E12.5 and E15.5 were fixed by immersion with 4% paraformaldehyde solution (PFA) in phosphate buffer saline (PBS) (pH 7.4) for 4 h at 4°C; between E15.5 and E18.5 days, embryos were perfused and postfixed for 6 h with the same fixative. The brains were dissected out and cryoprotected according to Bloch-Gallego et al. (1999). The frontal sections (20 µm thick) were collected using a cryostat on parallel sets of SuperFrost Plus slides (Thermo Scientific, J1800AMNZ) and stored at −80°C until use.

Isolation of MEFs from *Trio*$^{+/-}$ littermates

MEFs could be prepared from E14.5 and E18.5 using an eviscerated individual embryo freed of blood vessels or the skin of the back for older embryos. Tissues were trypsinized (0.25%) at 37° for one hour, dissociated and centrifuged quickly. The supernatant was collected and seeded in Dulbecco's Modified Eagle Medium (Life Technologies)/10% foetal calf serum (FCS), 1% penicillin/streptomycin (100 UI/ml). The pellet was trypsinized for 1 h longer. The previous steps were repeated until most tissues were dissociated.

Primary cultures of E13 thalamic neurons

Coronal slices of different levels of WT and *Trio*$^{-/-}$ mice at E13.5 were prepared as described by López-Bendito et al. (2006). Thalamic tissues were dissected from these slices, dissociated by trypsin-EDTA 0.05% (Invitrogen) for 15 min at 37°C and cultured on wells coated with poly-L-ornithine/laminin (both from Sigma-Aldrich) in neurobasal medium supplemented with B27 1×, N2 1× (both from Gibco, Thermo Fisher Scientific), 20 mM glucose (Sigma-Aldrich), 2 mM glutamine and penicillin-streptomycin 1× (both from Invitrogen) for 24-36 h.

Collapse assay

Dissociated cultures from thalamic neurons at E13.5 were performed as described in Deck et al. (2013). After 24 h of culture, neurons were incubated with commercial mouse-Slit2 at a 2 µg/ml final concentration (R&D Systems Europe, 5444-SL-050) for 20 min at 37°C, fixed, immunostained with mouse anti-β-tubulin antibody (Tuj1, 1:200, Sigma-Aldrich), and labelled with Texas Red-X or Alexa Fluor 488-Phalloidin (1:200, Molecular Probes, Thermo Fisher Scientific) to analyse growth cone morphologies. Collapsed growth cones were scored as in Castellani et al. (2000).

Immunohistochemistry and antibodies

Immunochemistry was performed on vibratome sections. After fixation, the brains were dissected out, embedded in agarose 4% in PBS and cut into 100 µm thick sections with a vibratome. Free floating sections were saturated in PBS, 10% FCS, 0.1% triton. The immunostaining was performed with rat anti-L1 1:200 (Millipore, MAB5272) overnight at room temperature. The primary antibody was revealed using secondary anti-rat antibody conjugated to donkey anti-mouse Alexa 488 or donkey anti-mouse Alexa 546 (1:1000, Life Technologies, A21202 or A10036, respectively). Once the immunoreactions were performed, the sections were treated with DAPI (1 mg/ml, Vector).

ISH and RNA probes

ISH was performed on 20 µm thick cryosections according to Bloch-Gallego et al. (1999). We linearized the mouse *Trio* subclone (MT7 for all *Trio* isoforms, Backer et al., 2007) with *NotI* (Invitrogen) enzymes and used T7 RNA polymerase (Roche). We synthesized from mouse E14 telencephalon cDNA a probe that corresponded to the Trio-GEF2 domain using the following primers together with the T7 polymerase by RT-PCR: forward AGGCACTATGTTTTGCAAGAG; reverse CCAC-GTTTGCCGGACGCT. We linearized the mouse *Ebf1* subclone with *Xba1* (Invitrogen) enzymes and used T3 RNA polymerase (Bielle et al., 2011).

Dosage of the endogenous RhoA or Rac1 activity in ventral telencephalic explants or MEFs

Freshly dissected ventral telencephalon or MEFs were lysed with ice-cold lysis buffer [25 mM Tris-HCl (pH 7.5), 1% NP40, 100 mM NaCl, 10 mM $MgCl_2$, 5% glycerol, 5 mM NaF, 1 mM phenylmethylsulfonyl fluoride (PMSF), 1 µl/ml protease inhibitor cocktail (Sigma-Aldrich)] and clarified by centrifugation at 1600 ***g*** for 5 min at 4°C. To evaluate RhoA activity, 300 µg of the protein lysate was incubated with 50 µg of Rhotekin-RBD beads (Cytoskeleton), for 1 h at 4°C for RhoA, or with 100 mg of glutathione S-transferase (GST)-fusion protein containing the CRIB domain of the human p21 activated kinase 1 protein (PAK) (GST-PAK) attached to beads (Sigma) for Rac1. Bead pellets were washed 2× with 25 mM Tris-HCl (pH 7.5), 0.5% NP40, 40 mM NaCl, 30 mM $MgCl_2$, 1 mM dithiothreitol (DTT), 1 mM PMSF, 1 µl/ml protease inhibitor cocktail (Sigma-Aldrich) before addition of 5× Laemmli buffer.

Fractions were analysed by western blotting. Proteins were separated on a 12% SDS polyacrylamide gel and transferred onto a polyvinylidene difluoride membrane (GE Healthcare) for RhoA and onto a nitrocellulose membrane for Rac1. Blots were probed with either mouse monoclonal anti-RhoA (1:200, Santa Cruz Biotechnology, 26C4) or anti-Rac1 (1:1000, Transduction Laboratories, 610650).

The band density was quantified by Fusion software (Vilber Lourmat). The relative densities of pulled down RhoA were normalized to the total RhoA, in the same sample. Averages were analysed and standard deviations (s.d.) were calculated. Differences were considered as significant when $P<0.05$ using the Student's *t*-test.

Axonal tracing

After intracardiac perfusion with 4% PFA in 0.12 M phosphate buffer (pH 7.4), embryonic dissected brains were fixed at least overnight at 4°C in 4% PFA. Small crystals of DiI (D282, Molecular Probes, Invitrogen) and/or DiA (D291, Molecular Probes, Invitrogen) were inserted into the thalamus of E16.5 (for anterograde tracings) or the neocortex of E18.5 (for retrograde tracings) after hemidissection of the brains, and left to diffuse at 37°C (from 1-3 weeks in the dark). The status of the dye diffusion was assessed by whole-brain examination under the fluorescent binocular set-up (Leica MZ16F).

Subsequently, brains were embedded in 3% agarose and cut at a thickness of 80 µm with a vibratome. Hoechst (Sigma-Aldrich) was used for fluorescent nuclear counterstaining. The sections were mounted in PBS, observed and photographed using a Leica DM5500B microscope and a Hamamatsu ORCA-ER camera with appropriate filters.

Cell lines stimulation by Slit-2

After serum starvation and before use, primary MEFs were cultured in the presence of 3 days *in vitro*-conditioned medium from EBNA 293 cells secreting *Xenopus* Slit (EBNA-slit; Wu et al., 1999; Chen et al., 2000) fused in frame at its C terminus to a myc tag (Li et al., 1999). The *Xenopus* Slit is an orthologue of the mouse and human *Slit2* genes (Li et al., 1999). The efficiency of the commercially available mouse Slit2 and of conditioned medium from cells that stably secrete *Xenopus* Slit was equivalent. Note that MEFs from control and *Trio*$^{-/-}$ embryos express Robo1 and Robo2 endogenously as illustrated in Fig. S1A, and that Trio is totally absent in *Trio*$^{-/-}$ MEFs (Fig. S1A).

Immunoprecipitation and western blot

Lysates were prepared from MEFs. Cells were washed with ice-cold PBS and lysed in buffer containing 25 mM Tris-HCl (pH 7.5), 100 mM NaCl, 1 mM EDTA, 1 mM DTT, 1 mM PMSF, 2% Triton, for 15 min on ice and centrifuged at 16,000 ***g*** for 30 min at 4°C. Proteins were boiled with the Laemmli loading buffer, resolved on a 6% polyacrylamide gel and blotted on to nitrocellulose membrane (Amersham). After saturation in TBST [Tris-buffered saline (pH 7.6) containing 0.1% Tween 20] with 5% milk, membranes were incubated with the following primary antibodies: anti-Robo1 (a kind gift from F. Murakami, Osaka, Japan, 1:1000), anti-Robo2 (a kind gift from F. Murakami, Osaka, Japan, 1:3000; Andrews et al., 2006), anti-Trio (clone H120, Santa Cruz Laboratories, 1:200). Primary antibodies were revealed by incubation with mouse anti-rabbit IgG-HRP or mouse anti-goat IgG-HRP (sc-2357 or sc-2354, respectively, Santa Cruz Laboratories, 1:25,000). Bands were revealed with Femto ECL (Thermo Scientific Pierce Protein Biology).

Statistical analysis

Quantitative data sets were analysed using a two-way ANOVA with Bonferroni's multiple comparison test (Fig. 1A) using GraphPad Prism 6 software, and a Student *t*-test (Fig. 1B). For quantifications of collapse assays (Fig. 6M), a Fisher's exact test was performed using GraphPad

Prism software to determine whether the qualitative variables (collapsed and non-collapsed growth cones/with or without Slit2 stimulation) were independent. Statistical significance were set at $*P<0.05$, $**P<0.01$ and $****P<0.0001$. $P>0.05$ was not significant (ns).

Acknowledgements
We thank Christine Métin, Serge Marty, Valérie Doye and Jérôme Delon for their helpful suggestions and critical reading of the manuscript. We also thank Luis Puelles for his advice in neuroanatomy. We would like to thank Annie Goldman for English proofreading.

Competing interests
The authors declare no competing or financial interests.

Author contributions
Conceptualization: S.B., S.G., E.B.-G.; Methodology: S.B., L.L.; Validation: S.B., L.L., C.L.; Formal analysis: S.B., L.L., S.G., E.B.-G.; Investigation: S.B., L.L., M.D., E.B.-G.; Writing - original draft: L.L., E.B.-G.; Writing - review & editing: L.L., S.G., E.B.-G.; Visualization: S.B., L.L., E.B.-G.; Supervision: E.B.-G.; Project administration: E.B.-G.; Funding acquisition: E.B.-G.

Funding
This research was supported by the Institut National de la Santé et de la Recherche Médicale and the Fondation pour la Recherche Médicale (contract N° DCM20111223066) to E.B.-G. This work was also funded by the European Research Council consolidator grant NImO616080 to S.G.

Supplementary information
Supplementary information available online at
http://dev.biologists.org/lookup/doi/10.1242/dev.153692.supplemental

References
Andrews, W., Liapi, A., Plachez, C., Camurri, L., Zhang, J., Mori, S., Murakami, F., Parnavelas, J. G., Sundaresan, V. and Richards, L. J. (2006). Robo1 regulates the development of major axon tracts and interneuron migration in the forebrain. *Development* **133**, 2243-2252.

Ba, W., Yan, Y., Reijnders, M. R. F., Schuurs-Hoeijmakers, J. H. M., Feenstra, I., Bongers, E. M. H. F., Bosch, D. G. M., De Leeuw, N., Pfundt, R., Gilissen, C. et al. (2016). TRIO loss of function is associated with mild intellectual disability and affects dendritic branching and synapse function. *Hum. Mol. Genet.* **25**, 892-902.

Backer, S., Hidalgo-Sanchez, M., Offner, N., Portales-Casamar, E., Debant, A., Fort, P., Gauthier-Rouviere, C. and Bloch-Gallego, E. (2007). Trio controls the mature organization of neuronal clusters in the hindbrain. *J. Neurosci.* **27**, 10323-10332.

Bellanger, J.-M., Lazaro, J.-B., Diriong, S., Fernandez, A., Lamb, N. and Debant, A. (1998). The two guanine nucleotide exchange factor domains of Trio link the Rac1 and the RhoA pathways in vivo. *Oncogene* **16**, 147-152.

Bielle, F., Marcos-Mondejar, P., Keita, M., Mailhes, C., Verney, C., Nguyen Ba-Charvet, K., Tessier-Lavigne, M., Lopez-Bendito, G. and Garel, S. (2011). Slit2 activity in the migration of guidepost neurons shapes thalamic projections during development and evolution. *Neuron* **69**, 1085-1098.

Blangy, A., Vignal, E., Schmidt, S., Debant, A., Gauthier-Rouviere, C. and Fort, P. (2000). TrioGEF1 controls Rac- and Cdc42-dependent cell structures through the direct activation of rhoG. *J. Cell Sci.* **113**, 729-739.

Bloch-Gallego, E., Ezan, F., Tessier-Lavigne, M. and Sotelo, C. (1999). Floor plate and netrin-1 are involved in the migration and survival of inferior olivary neurons. *J. Neurosci.* **19**, 4407-4420.

Braisted, J. E., Catalano, S. M., Stimac, R., Kennedy, T. E., Tessier-Lavigne, M., Shatz, C. J. and O'Leary, D. D. M. (2000). Netrin-1 promotes thalamic axon growth and is required for proper development of the thalamocortical projection. *J. Neurosci.* **20**, 5792-5801.

Briancon-Marjollet, A., Ghogha, A., Nawabi, H., Triki, I., Auziol, C., Fromont, S., Piche, C., Enslen, H., Chebli, K., Cloutier, J.-F. et al. (2008). Trio mediates netrin-1-induced Rac1 activation in axon outgrowth and guidance. *Mol. Cell. Biol.* **28**, 2314-2323.

Castellani, V., Chédotal, A., Schachner, M., Faivre-Sarrailh, C. and Rougon, G. (2000). Analysis of the L1-deficient mouse phenotype reveals cross-talk between Sema3A and L1 signaling pathways in axonal guidance. *Neuron* **27**, 237-249.

Castillo-Paterna, M., Moreno-Juan, V., Filipchuk, A., Rodriguez-Malmierca, L., Susin, R. and Lopez-Bendito, G. (2015). DCC functions as an accelerator of thalamocortical axonal growth downstream of spontaneous thalamic activity. *EMBO Rep.* **16**, 851-862.

Causeret, F., Hidalgo-Sanchez, M., Fort, P., Backer, S., Popoff, M. R., Gauthier-Rouviere, C. and Bloch-Gallego, E. (2004). Distinct roles of Rac1/Cdc42 and Rho/Rock for axon outgrowth and nucleokinesis of precerebellar neurons toward netrin 1. *Development* **131**, 2841-2852.

Chen, J.-H., Wu, W., Li, H.-S., Fagaly, T., Zhou, L., Wu, J. Y. and Rao, Y. (2000). Embryonic expression and extracellular secretion of Xenopus slit. *Neuroscience* **96**, 231-236.

Chen, Z. (2018). Common cues wire the spinal cord: Axon guidance molecules in spinal neuron migration. *Semin. Cell Dev. Biol.* (in press).

Cherfils, J. and Zeghouf, M. (2013). Regulation of small GTPases by GEFs, GAPs, and GDIs. *Physiol. Rev.* **93**, 269-309.

Debant, A., Serra-Pages, C., Seipel, K., O'Brien, S., Tang, M., Park, S. H. and Streuli, M. (1996). The multidomain protein Trio binds the LAR transmembrane tyrosine phosphatase, contains a protein kinase domain, and has separate rac-specific and rho-specific guanine nucleotide exchange factor domains. *Proc. Natl. Acad. Sci. USA* **93**, 5466-5471.

Deck, M., Lokmane, L., Chauvet, S., Mailhes, C., Keita, M., Niquille, M., Yoshida, M., Yoshida, Y., Lebrand, C., Mann, F. et al. (2013). Pathfinding of corticothalamic axons relies on a rendezvous with thalamic projections. *Neuron* **77**, 472-484.

DeGeer, J., Boudeau, J., Schmidt, S., Bedford, F., Lamarche-Vane, N. and Debant, A. (2013). Tyrosine phosphorylation of the Rho guanine nucleotide exchange factor Trio regulates netrin-1/DCC-mediated cortical axon outgrowth. *Mol. Cell. Biol.* **33**, 739-751.

DeGeer, J., Kaplan, A., Mattar, P., Morabito, M., Stochaj, U., Kennedy, T. E., Debant, A., Cayouette, M., Fournier, A. E. and Lamarche-Vane, N. (2015). Hsc70 chaperone activity underlies Trio GEF function in axon growth and guidance induced by netrin-1. *J. Cell Biol.* **210**, 817-832.

Di Donato, N., Jean, Y. Y., Maga, A. M., Krewson, B. D., Shupp, A. B., Avrutsky, M. I., Roy, A., Collins, S., Olds, C., Willert, R. A. et al. (2016). Mutations in CRADD result in reduced caspase-2-mediated neuronal apoptosis and cause megalencephaly with a rare lissencephaly variant. *Am. J. Hum. Genet.* **99**, 1117-1129.

Fouquet, C., Di Meglio, T., Ma, L., Kawasaki, T., Long, H., Hirata, T., Tessier-Lavigne, M., Chedotal, A. and Nguyen-Ba-Charvet, K. T. (2007). Robo1 and robo2 control the development of the lateral olfactory tract. *J. Neurosci.* **27**, 3037-3045.

Jaffe, A. B. and Hall, A. (2005). Rho GTPases: biochemistry and biology. *Annu. Rev. Cell Dev. Biol.* **21**, 247-269.

Katrancha, S. M., Wu, Y., Zhu, M., Eipper, B. A., Koleske, A. J. and Mains, R. E. (2017). Neurodevelopmental disease-associated de novo mutations and rare sequence variants affect TRIO GDP/GTP exchange factor activity. *Hum. Mol. Genet.* **26**, 4728-4740.

Lawson, C. D. and Burridge, K. (2014). The on-off relationship of Rho and Rac during integrin-mediated adhesion and cell migration. *Small GTPases* **5**, e27958.

Li, H.-S., Chen, J.-H., Wu, W., Fagaly, T., Zhou, L., Yuan, W., Dupuis, S., Jiang, Z.-H., Nash, W., Gick, C. et al. (1999). Vertebrate slit, a secreted ligand for the transmembrane protein roundabout, is a repellent for olfactory bulb axons. *Cell* **96**, 807-818.

Liu, X., Lu, Y., Zhang, Y., Li, Y., Zhou, J., Yuan, Y., Gao, X., Su, Z. and He, C. (2012). Slit2 regulates the dispersal of oligodendrocyte precursor cells via Fyn/RhoA signaling. *J. Biol. Chem.* **287**, 17503-17516.

Lokmane, L. and Garel, S. (2014). Map transfer from the thalamus to the neocortex: inputs from the barrel field. *Semin. Cell Dev. Biol.* **35**, 147-155.

Lokmane, L., Proville, R., Narboux-Nême, N., Györy, I., Keita, M., Mailhes, C., Léna, C., Gaspar, P., Grosschedl, R. and Garel, S. (2013). Sensory map transfer to the neocortex relies on pretarget ordering of thalamic axons. *Curr. Biol.* **23**, 810-816.

Long, H., Yoshikawa, S. and Thomas, J. B. (2016). Equivalent activities of repulsive axon guidance receptors. *J. Neurosci.* **36**, 1140-1150.

López-Bendito, G., Cautinat, A., Sánchez, J. A., Bielle, F., Flames, N., Garratt, A. N., Talmage, D. A., Role, L. W., Charnay, P., Marín, O. et al. (2006). Tangential neuronal migration controls axon guidance: a role for neuregulin-1 in thalamocortical axon navigation. *Cell* **125**, 127-142.

McMullan, R., Anderson, A. and Nurrish, S. (2012). Behavioral and immune responses to infection require Galphaq- RhoA signaling in C. elegans. *PLoS Pathog.* **8**, e1002530.

Nakamura, F. (2013). FilGAP and its close relatives: a mediator of Rho-Rac antagonism that regulates cell morphology and migration. *Biochem. J.* **453**, 17-25.

Nguyen-Ba-Charvet, K. T., Plump, A. S., Tessier-Lavigne, M. and Chédotal, A. (2002). Slit1 and slit2 proteins control the development of the lateral olfactory tract. *J. Neurosci.* **22**, 5473-5480.

O'Brien, S. P., Seipel, K., Medley, Q. G., Bronson, R., Segal, R. and Streuli, M. (2000). Skeletal muscle deformity and neuronal disorder in Trio exchange factor-deficient mouse embryos. *Proc. Natl. Acad. Sci. USA* **97**, 12074-12078.

Plageman, T. F., Jr, Chauhan, B. K., Yang, C., Jaudon, F., Shang, X., Zheng, Y., Lou, M., Debant, A., Hildebrand, J. D. and Lang, R. A. (2011). A Trio-RhoA-Shroom3 pathway is required for apical constriction and epithelial invagination. *Development* **138**, 5177-5188.

Portales-Casamar, E., Briançon-Marjollet, A., Fromont, S., Triboulet, R. and Debant, A. (2006). Identification of novel neuronal isoforms of the Rho-GEF Trio. *Biol. Cell* **98**, 183-193.
Powell, A. W., Sassa, T., Wu, Y., Tessier-Lavigne, M. and Polleux, F. (2008). Topography of thalamic projections requires attractive and repulsive functions of Netrin-1 in the ventral telencephalon. *PLoS Biol.* **6**, e116.
Sadybekov, A., Tian, C., Arnesano, C., Katritch, V. and Herring, B. E. (2017). An autism spectrum disorder-related de novo mutation hotspot discovered in the GEF1 domain of Trio. *Nat. Commun.* **8**, 601.
Schmidt, S. and Debant, A. (2014). Function and regulation of the Rho guanine nucleotide exchange factor Trio. *Small GTPases* **5**, e29769.
Settleman, J. (2003). A nuclear MAL-function links Rho to SRF. *Mol. Cell* **11**, 1121-1123.
Tcherkezian, J. and Lamarche-Vane, N. (2007). Current knowledge of the large RhoGAP family of proteins. *Biol. Cell* **99**, 67-86.
Wong, K., Ren, X.-R., Huang, Y.-Z., Xie, Y., Liu, G., Saito, H., Tang, H., Wen, L., Brady-Kalnay, S. M., Mei, L. et al. (2001). Signal transduction in neuronal migration: roles of GTPase activating proteins and the small GTPase Cdc42 in the Slit-Robo pathway. *Cell* **107**, 209-221.
Wu, W., Wong, K., Chen, J., Jiang, Z., Dupuis, S., Wu, J. Y. and Rao, Y. (1999). Directional guidance of neuronal migration in the olfactory system by the protein Slit. *Nature* **400**, 331-336.